Dynamics and Ordering in the Columnar Mesophases of Octa-alkyloxy Orthocylophane: A Carbon-13 NMR Investigation

Ramaswamy Kannan,[†] Tapas Sen,[†] Raphy Poupko,[†] Zeev Luz,*[,†] and Herbert Zimmermann[‡]

Weizmann Institute of Science, Rehovot 76100, Israel, and Max-Planck-Institut für Medizinische Forschung, Jahnstrasse 29, 69120 Heidelberg, Germany

Received: June 26, 2003

Octa-alkyloxy tetrabenzo-orthocyclophanes (TBC-*n* where *n* is the number of carbons in the side chains) exhibit columnar mesophases of various symmetries, depending on the length of the side chains. The conformation of the orthocylophane core in these mesophases is that of a sofa, with the molecules stacking on top of each other to form columns. Within these columns, the molecules undergo reorientation via a combined pseudorotation/rotation mechanism. In the present work, carbon-13 NMR is used to study the mechanism and the kinetic parameters of this process, as well as the ordering characteristics in two homologues of the series, viz. TBC-9, which exhibits a single rectangular mesophase (Dr), and TBC-12, which is polymorphic with two mesophases, a low-temperature Dr and a high-temperature hexagonal columnar phase, Dh. Using 1D and 2D dynamic carbon-13 MAS NMR, the pseudorotation/rotation mechanism suggested earlier by Kuebler et al. on the basis of deuterium NMR studies (*Liq. Cryst.* **1995**, *18*, 300) is confirmed and kinetic parameters for the process are derived. Where comparable, the results are consistent with the earlier measurements. The results also indicate the presence of fast high-amplitude librations of the sofa conformation within the columns. The NMR lines of the MAS spectra within the mesophases are inhomogeneously broadened due to the distribution of isotropic chemical shifts. The latter probably reflects packing heterogeneity along the columns. Dynamic measurements of the sofa-sofa pseudorotation of TBC-9 in chloroform solutions are also reported.

1. Introduction

The molecules of most discotic liquid crystals consist of rigid flat cores with laterally linked flexible side chains.[1] This structure allows easy reorientation of the molecules within the columns of discotic columnar mesophases. The core flatness facilitates the slipping of the molecules relative to each other, whereas the side chains provide "lubrication" for the reorientational motion. Yet, there are certain classes of discotic mesogens in which the molecular core is not flat (for example, derivatives of tribenzocyclononene[2,3]) and not even rigid. To the latter class belong the mesogens derived from tetrabenzo-orthocyclophanes[4−9] (Figure 1a).

This core can acquire several flexible conformations (see part c of the figure) of which the sofa is the most stable one.[9,10] When substituted with eight, sufficiently long, alkyloxy or alkanoyloxy side chains, the compounds are mesogenic, exhibiting columnar mesophases of different symmetries. The mesomorphic properties of several homologues of these series were studied by differential scanning calorimetry (DSC), optical polarizing microscopy, X-ray diffraction, and deuterium NMR.[4−9] The latter work[9] describes a detailed analysis of the deuterium NMR spectrum of one member (octa-heptyloxy) of the series in terms of the motional and ordering characteristics in the mesophase region. It confirms that the core conformation in the mesophase is most likely that of a sofa and that in the columns the molecules are stacked on top of each other in a locked form, like in a pile of chairs (see Figure 2a).

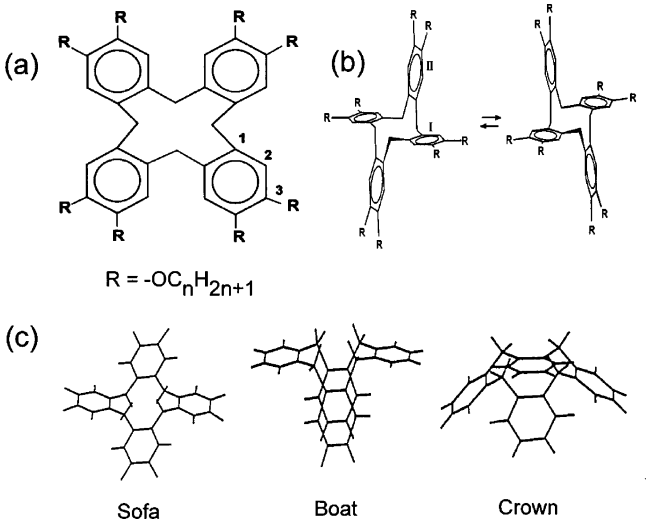

Figure 1. (a) Structural formula of the octa-alkyloxy orthocyclophane (TBC-*n*) with the numerical convention used for the aromatic carbons. (b) The sofa-sofa interconversion (pseudorotation) process and the labeling of the benzene rings in the flat (I) and perpendicular (II) parts of the sofa conformation. (c) The sofa, boat, and crown conformations of the TBC core.

Furthermore, on the basis of the deuterium NMR spectra, two modes of motions within the columns have been identified. One consists of rapid (on the NMR time scale) high-amplitude librations involving two (or more) distorted sofa forms. Molecular models show that the sofa conformation is highly flexible so that such distorted forms could readily be obtained by right and left twists of the C_{2h} conformation about the Z_{MF}

* To whom correspondence should be addressed.
[†] Weizmann Institute of Science.
[‡] Max-Planck-Institut für Medizinische Forschung.

10.1021/jp030793m CCC: $25.00
Published on Web 10/30/2003

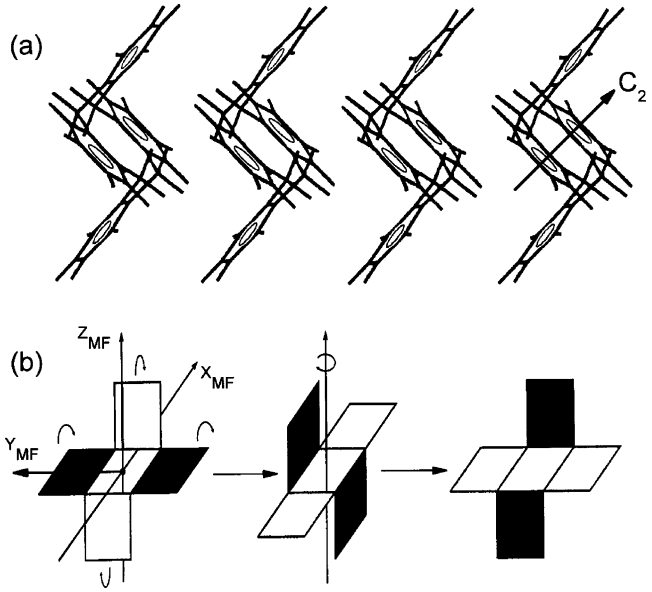

Figure 2. (a) Schematic diagram showing the stacking of the TBC-*n* molecules in the columns. The C_2 axis of the core of one molecule (assumed to possess an ideal C_{2h} symmetry) is indicated on the rightmost molecule. (b) The pathway of the pseudorotation/rotation process in the columns (adapted from Kuebler et al.[9]). The molecular frame (MF) used in the text is shown for the leftmost diagram.

axis (see Figure 2b) into ones with C_i symmetry. The other motion corresponds to an axial reorientation of the molecule without changing their stacking ordering. It involves a concerted pseudorotation/rotation mechanism as shown in part b of the figure. Additional (unpublished) work on three more tetrabenzocyclophane derivatives is described in the Ph.D. Dissertation of Kuebler.[11]

In the present paper, we extend these studies in two ways. First, we use carbon-13 MAS NMR spectroscopy in order to extend the dynamic range of the deuterium measurements and to provide an independent confirmation of the proposed mechanisms. Second, we extend the measurements to two other homologues of the alkyloxy series (henceforth referred to as TBC-*n*, where *n* is the number of carbons in the side chains). One is TBC-9 which, like TBC-7, exhibits a single columnar rectangular mesophase, Dr (center rectangular with *C*2*mm* symmetry). The second compound is the polymorphic mesogen TBC-12 with a low-temperature Dr phase and a high-temperature hexagonal, Dh, mesophase (with *p*6*mm* symmetry). The phase diagrams of the two compounds are[6]

$$\text{TBC}-9: \quad C_2 \xrightarrow{97.6\ ^\circ\text{C}} C_1 \xrightarrow{109.4\ ^\circ\text{C}} \text{Dr} \xrightarrow{147.9\ ^\circ\text{C}} \text{Iso}$$

$$\text{TBC}-12: \quad C_2 \xrightarrow{78.1\ ^\circ\text{C}} C_1 \xrightarrow{94.4\ ^\circ\text{C}} \text{Dr} \xrightarrow{121.5\ ^\circ\text{C}} \text{Dh} \xrightarrow{133.2\ ^\circ\text{C}} \text{Iso}$$

where Iso stands for the isotropic melt, and C_1 and C_2 are two solid phases (both compounds have another solid phase below room temperature). Note the change in nomenclature for the columnar phases from D_1 and D_2 in Spielberg et al.[6] to Dr and Dh, respectively, in the present paper. The Dr ↔ Dh transition involves a small discontinuous change in the lattice parameters of the two-dimensional array of columns.[6] The transition is clearly observed by optical microscopy but not in the DSC thermogram. It thus appears to be weakly first order.

Carbon-13 MAS NMR has been used earlier for studying discotic mesophases. Thus, Khetrapal et al.[12] used this method to study the solid underlying the discotic mesophase of hexa octanoyloxy benzene, and Akai et al.[13] applied it to investigate the chain melting in the mesophases of a porphyrin derivative. More recently Fischbach et al.[14] and Zimmermann et al.[3] applied dynamic carbon-13 methods to study the structure and motions in the columnar mesophases derived from, respectively, hexabenzocoronene and tribenzocyclononatriene. Finally, Dvinskikh et al.[15] used carbon-13 NMR to extend an earlier deuterium NMR study[16] of the discotic mesophases of substituted rufigallol.

To become familiar with the carbon-13 spectra of the TBC-*n* compounds and their flexible nature, we first studied some of them in solution and analyzed their temperature-dependent NMR spectra in terms of the sofa-sofa pseudorotation dynamics. This process was studied earlier by White and Gesner[17] in the parent homologue of the series (TBC-1) using proton NMR. We then describe the carbon-13 MAS spectrum of TBC-9 in the solid and Dr phases, followed by complementary deuterium NMR measurements on a specifically deuterated isotopologue of this compound. Finally, we extend the results to the polymorphic homologue, TBC-12. Where comparable, the results are consistent with the earlier deuterium studies;[9,11] however, there are certain aspects where carbon-13 NMR provides additional information. We discuss the merits and limitation of the technique vis-à-vis those of using deuterium NMR.

2. Experimental Section

The carbon-13 measurements were done on isotopically normal compounds, whereas the deuterium measurements were performed on isotopologues labeled in the unsubstituted aromatic sites. We refer to these isotopologues as TBC-$n-d_8$. The synthesis of all these compounds was as described earlier.[4,6,8,9]

The high-resolution variable-temperature carbon-13 NMR measurements were carried out on a Bruker DRX-400 spectrometer operating at 100.3 MHz. For the solid state deuterium (static samples) and carbon-13 MAS (and partly on static samples) measurements, a Bruker DSX-300 spectrometer was used at 46.07 and 75.47 MHz, respectively. The MAS spectra were recorded by cross-polarization (CP) using a contact time of 2 ms. The MAS samples were contained in 4 mm rotors, and the temperature was calibrated using lead nitrate. Some carbon-13 MAS experiments were also performed at 201 MHz, using a Bruker DRX800 spectrometer equipped with a suitable magic angle spinning probe. Other details are as described in Zimmermann et al.[3]

3. High-Resolution Carbon-13 NMR Spectra in Solution

In Figure 3 are shown high-resolution carbon-13 NMR spectra of a solution of TBC-9 in chloroform as a function of the temperature. The spectra below about −20 °C are consistent with a nonrearranging sofa conformation with C_{2h} symmetry. The low-field signals (110−150 ppm) are due to the aromatic carbons, those around 69 and 34.5 ppm correspond to the α-CH_2 (of the side chains) and ring-CH_2 carbons, respectively, whereas the other high-field signals are assigned to the rest of the aliphatic carbons in the side chains. From the structure and average symmetry of the sofa conformation, we expect one peak for the ring-CH_2 and two sets of signals for each type of the aromatic (I and II) and side chain carbons (see Figure 1). Doubling of the signals is indeed observed for the aromatic and the α-methylene carbons, but the resolution is apparently not sufficient to discriminate the signals of the other side chain carbons. On the basis of chemical shift additivity rules,[18] the three doublets in the aromatic region of the spectrum (110−150 ppm) can be assigned (from low to high field) to the C−O

TABLE 1: Chemical Shift Parameters (in ppm) of the Aromatic Carbons of TBC-9 in Various Phases

phase	carbon no.	δ_{iso}	δ_{11}^{PAS}	δ_{22}^{PAS}	δ_{33}^{PAS}	$\Delta\delta^d$
solution (−30 °C)[a]	1 (C−C)	131.8/132.8				
melt (133 °C)		133.1				
C_2 solid (20 °C)[b]		130	92	28	−120	212
Dr mesophase (117 °C)[c]		131	72	30	−102	173
solution (−30 °C)[a]	2 (C−H)	111.7/116.9				
melt (133 °C)		118.9				
C_2 solid (20 °C)[b]		108	81	24	−105	186
Dr mesophase (117 °C)[c]		114/117	68/76	14/2	−82/−78	150/154
solution (−30 °C)[a]	3 (C−O)	147.0/147.5				
melt (133 °C)		149.1				
C_2 solid (20 °C)[b]		146	72	11	−83	155
Dr mesophase (117 °C)[c]		147	45	22	−67	112

[a] $CDCl_3$. [b] The results apply to the sharp singlets in the spectra. [c] Measured just above the melting temperature. [d] $\Delta\delta = \delta_{11}^{PAS} - \delta_{33}^{PAS}$.

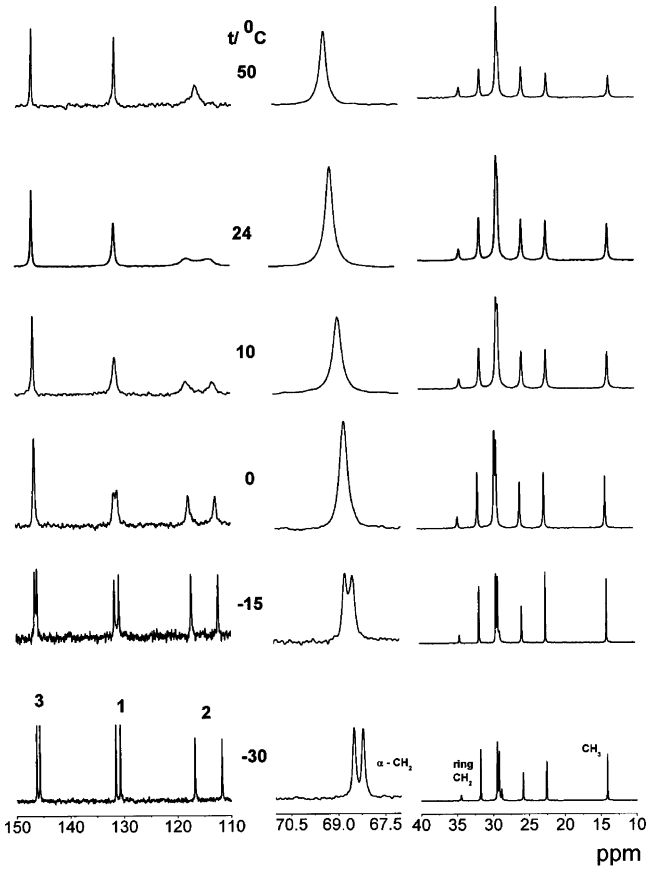

Figure 3. High-resolution carbon-13 NMR spectra (at 100.3 MHz) of a $CDCl_3$ solution of TBC-9 at the indicated temperatures. Peak assignments of some of the carbons are given on the bottom trace. Note the different scales used for the different regions of the spectra.

(number 3 in Figure 2a), C−C (1), and C−H (2) carbons, as indicated in the bottom trace of Figure 3. For later purposes, the chemical shifts of the aromatic carbons are summarized in Table 1.

As the temperature is raised to above −20 °C gradual line broadening of the signals due to the aromatic and α-methylene signals take place, reflecting the setting-in of the sofa-sofa pseudorotation process (Figure 1b). On further heating, the corresponding pairs of lines coalesce and eventually merge to singlets. The low-field part of the 24 °C spectrum is similar to that of TBC-1 in chloroform recorded by Burlinson and Ripmeester at room temperature.[19] A quantitative analysis of such line shapes (combined with similar high-resolution proton NMR measurements) in terms of the rate of the sofa-sofa interconversion process yields the Arrhenius plot shown in

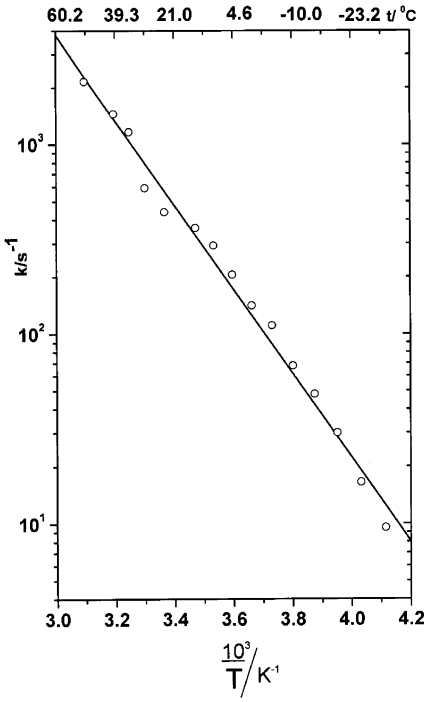

Figure 4. Arrhenius plot of the rate constants for the sofa-sofa interconversion of TBC-9 in a chloroform solution. The data include results from carbon-13 (as in Figure 3) as well as from high-resolution proton measurements.

Figure 4 with the following kinetic parameters:

$$\log(A/s^{-1}) = 10.22 \pm 0.24; \quad \Delta E = 42.4 \pm 1.3 \text{ kJ mol}^{-1};$$
$$\Delta S = -56.9 \pm 4.6 \text{ J K}^{-1} \text{ mol}^{-1}$$

These values are essentially the same as those measured by White and Gesner[17] for TBC-1, k(300 K) = 890 s^{-1}; $\log(A/s^{-1}) = 11.0$; $\Delta E = 46.8$ kJ mol^{-1}; $\Delta S = -43.4$ J K^{-1} mol^{-1}. The negative activation entropy suggests that the intermediate state is more rigid than the sofa, perhaps corresponding to a distorted crown or a flattened boat conformation.[10]

4. TBC-9 NMR Spectra in the Solid and Mesophase

4.1. Carbon-13 MAS and Deuterium Spectra. The main emphasis in the present study is on the dynamic properties of the TBC-*n* homologues in the columnar mesophases, as reflected in the carbon-13 MAS spectra. Before discussing these results, we briefly comment on the MAS spectra of the two solid phases underlying the mesophase and of the mesophase at the low-temperature end of its stability range. Examples are shown in Figure 5.

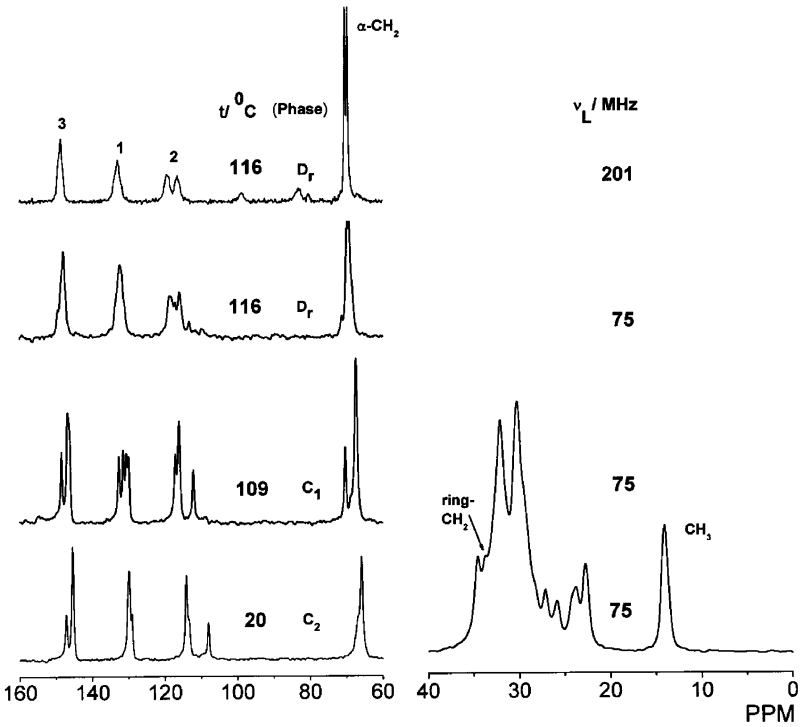

Figure 5. Carbon-13 MAS spectra of TBC-9. The bottom three spectra were recorded at a Larmor frequency of 75.47 MHz with a spinning frequency, $\nu_R = 6$ kHz, at the indicated temperatures and phases. Recycle time, 10 s; number of scans, 150−350. Top trace: The spectrum of the mesophase, as in the previous trace, but recorded at a Larmor frequency of 201 MHz with $\nu_R = 10$ kHz. Some of the peaks are identified on the bottom and top traces.

Referring first to the spectrum of the room-temperature solid, C_2, we can easily distinguish between the signals of the three types of aromatic carbons, the α-methylene, and the rest of the aliphatic carbons, by comparison with the solution spectrum (Figure 3). However, the structure of the spectrum, in particular in the aromatic region, is quite complicated. It appears to consist of a superposition of two subspectra with relative intensity 1:1. In the aromatic region, one subspectrum consists of three doublets, whereas the other consists of three singlets (partially overlapping with the former), each of which is double the intensity of the peaks in the first subspectrum. The most likely interpretation of this spectrum is in terms of a single sofa conformer in a crystallographic site of low symmetry. In fact the spectrum can be explained in terms of a local C_s (or nearly C_s) symmetry, so that a reflection plane, perpendicular to the long molecular axis (C_2 of the free sofa conformer), halves the molecule into two symmetric parts. The two benzene rings along the flat part of the sofa are then equivalent (giving rise to the three aromatic singlets), whereas the two perpendicular rings are in general not equivalent (giving rise to the three aromatic doublets). Transition to C_1 results in small shifts of the lines and some narrowing. The main effect is on the signals of carbon 1, which now exhibits four lines of equal intensities, indicating a lower symmetry than C_s, with all benzene rings nonequivalent. Similar, but less resolved, spectra were obtained for the solid phases of TBC-12, lending support for the above interpretation. The carbon-13 MAS spectra of the aromatic carbons of TBC-1 in the solid state[19] showed similar features as described above for the higher homologues.

Figure 5 also shows the MAS spectrum of the Dr mesophase recorded just a few degrees above the melting of C_1 (two top traces, corresponding to Larmor frequencies of 75 and 201 MHz). The spectrum recorded at 75 MHz was slightly bi-phasic, as evidenced by several weak, but sharp, features that match the positions of the more intense peaks in the spectrum of the underlying C_1 phase. The spectrum of the mesophase is consistent with a single, nonpseudorotating (or only slowly pseudorotating), sofa conformer. Under these conditions, we expect the signals of the aromatic and the α-methylene carbons to exhibit doublets, because of the two types of benzene rings in the symmetric sofa conformation. In effect, a clear splitting is observed for the C−H and (with a much lower resolution) also for the α-methylene signals, but no splitting is revealed by signals of the C−C and C−O carbons. The lack of splitting for the latter signal is evidently due to the much larger widths of the signals in the mesophase, in particular of the aromatic carbons, so that only the largest splitting of the C−H carbons is resolved.

The larger width of the signals in the mesophase (compared to that in the solid) is quite unusual. More commonly, the signals in the mesophase are narrower than those in the underlying solids, because of motional averaging effects in the former. An example of the latter is demonstrated by the carbon-13 MAS spectra of the solid and columnar mesophases in the related homologous series derived from tribenzocyclononene.[3] The larger line width observed in the Dr mesophase (compared to the solid) cannot be ascribed to dynamic effects, such as pseudorotation/rotation. As discussed in the next sections, at 116 °C, this process is too slow to cause observable broadening. Rather we believe that it is due to internal inhomogeneity within the columns, resulting in a distribution in the isotropic chemical shift and in turn to inhomogeneous line broadening. This conclusion is supported by measurements performed at a much higher Larmor frequency (201 MHz). A spectrum recorded at the same temperature exhibited essentially the same line shape for the aromatic carbons with only a minor increase in the resolution of the C−H signal (see top trace in Figure 5). This means that the line width scales with the chemical shift as would be expected for a broadening resulting from a chemical shift dispersion. This dispersion may reflect inhomogeneous stacking,

for example, from density modulation along the columns. Such an effect was proposed by de Gennes[20] to account for the packing incommensurability of the core and side chains in columnar discotic liquid crystals. The idea is that the optimal stacking distance of the core is smaller than that of the side chains. This mismatching may, under certain circumstances, lead to density modulation with alternating pinched and sparse regions in the columns and in turn to a distribution in isotropic chemical shifts of the core carbons. The density modulation hypotheses was invoked to explain certain features in the deuterium spectrum of the columnar phases in rufigallol derivatives.[16] Although the interpretation for the latter system is under dispute,[15] it may very well apply in the present case.

In Table 1 are summarized the isotropic chemical shifts, δ_{iso} (relative to TMS), of the aromatic carbons of TBC-9 as measured in the various spectra described above. These include (i) the low-temperature chloroform solution, (ii) the isotropic melt, (iii) the mesophase (just above the melting temperature), and (iv) the room-temperature solid, C_2 (only values for the more intense peaks of each carbon are given). We have also determined the full chemical shift tensors for the latter peaks as well as for the aromatic carbons in the low-temperature region of the mesophase. These were obtained by analyzing the spinning sideband (ssb) intensities of spectra recorded at low spinning rates.[21] The results for the principal values of the chemical shift tensors are included in Table 1. These values are given with respect to the corresponding δ_{iso}, so that $\delta_{11}^{PAS} + \delta_{22}^{PAS} + \delta_{33}^{PAS} = 0$, and we used the convention that $\delta_{11}^{PAS} > \delta_{22}^{PAS} > \delta_{33}^{PAS}$. Based on earlier work on the chemical shift tensors of aromatic carbons in rigid solid systems,[22] we can safely assume that the most shielded component, δ_{33}^{PAS}, corresponds to the direction normal to the benzene ring. The other two directions are not as well determined by the local symmetry. It is often the case that the least shielded component, δ_{11}^{PAS}, lies nearly radially along the C−X bond direction (X = C, H, O). In the following, we shall assume this situation to apply in the present case, so that δ_{22}^{PAS} lies in the plane of the benzene ring perpendicular to the C−X direction.

Comparing the chemical shift anisotropy, $\Delta\delta = \delta_{11}^{PAS} - \delta_{33}^{PAS}$, of corresponding carbons, we note a considerable reduction in $\Delta\delta$ on going from the solid to the mesophase. This reduction most likely reflects the effect of fast high-amplitude libration of the sofa conformation within the columns of the mesophase. The occurrences of these librations were proposed by Kuebler et al.[9] to account for the relatively large biaxiality of the deuterium quadrupole tensor in the mesophase of TBC-7. The process can be viewed as fast switching between right- and left-twisted sofas, resulting in partial averaging of the anisotropic magnetic tensors.

We have performed similar deuterium NMR measurements on a TBC-9 sample specifically deuterated in the unsubstituted aromatic site (TBC-9-d_8). Examples of spectra in the two solid phases and at several temperatures in the mesophase region are depicted in Figure 6. The spectra correspond to rigid or weakly dynamic (on the deuterium NMR time scale) powder samples. In the solid phases, they correspond to nearly axially symmetric quadrupole tensors ($\eta \sim 0.06$), with $\nu_Q = 3e^2qQ/4h = 133$ kHz, whereas in the mesophase, the spectra exhibit considerable biaxiality with ν_Q decreasing from 110 to 103 kHz and η increasing from 0.09 to 0.17 in the temperature range 120−140 °C. Like Kuebler et al., we attribute these changes to the high-amplitude librations of the sofa conformers in the mesophase. The same motion is also responsible for the discontinuous decrease of the carbon-13 chemical shift anisotropy during the solid → mesophase transition (see Table 1). Most likely, the anisotropy continues to change within the mesophase, but its extent is difficult to estimate from the exchange broadened MAS spectra. This motion affects both the directions and the principal values of the average chemical shift tensors, which are required for the line shape analysis to be described in the next section. They can, in principle, be calculated if the exact nature of the librational motion is known. For lack of such information, we shall use the original directions in the molecular frame (Figure 2b) and the principal values determined in the low-temperature region of the mesophase (Table 1).

4.2. 2D-Exchange Spectra, Confirmation of the Pseudorotation/Rotation Mechanism. The MAS spectrum of the mesophase shown in Figure 5 was recorded just a few degrees above the melting of the solid C_1. On further heating to above 120 °C within the mesophase, the peaks of the aromatic and α-methylene carbons (center bands and associated ssb) gradually broaden, until the clearing temperature is reached. Examples of spectra for the aromatic carbons are shown in Figure 7 for two different sample spinning rates.

It may be seen that the extent of broadening is different for different carbons and also depends on the spinning rate. Such broadening effects are characteristic of dynamic processes, but the full line shape evolution (broadening followed by narrowing) is not displayed by these spectra because it is interrupted by the clearing transition at 147.9 °C. The dynamic process responsible for the observed line broadening in the mesophase most likely involves the reorientation of the sofa molecules within the columns, i.e., the process suggested by Kuebler et al. to account for the deuterium 2D exchange spectra in TBC-7.[9] These spectra indicated that the exchange involves $\pi/2$ jumps of the (aromatic) C−D bond, and on this basis, the mechanism combining pseudorotation and rotation as shown in Figure 2b was proposed. It consists of pseudorotation (first step in the figure) and a quarter cycle rotation (second step) to accommodate the molecule in a properly stacked position in the column. The two steps most likely take place in concert. We note that this process leads to exchange between corresponding carbons in the two types of nonequivalent benzene rings of the sofa conformation.

To confirm that the line broadening observed in the carbon-13 MAS spectra indeed corresponds to the pseudorotation/rotation process, we performed a rotor-synchronized 2D exchange experiment on the same sample used for the 1D MAS measurements. For these experiments, the method of Veeman and co-workers,[23] producing magnitude spectra, was performed. Results, recorded at 75.45 MHz for several mixing times, τ_m, are shown in Figure 8. In the presence of exchange, such experiments may yield two types of cross-peaks.[24,25] One type, referred to as auto cross-peaks, link between the center and ssb of the same nuclei. Such cross-peaks indicate (physical) reorientation of the molecular moiety including the particular nucleus. The second type are hetero cross-peaks, which link between peaks associated with nonequivalent atoms. They indicate the presence of a chemical exchange (rearrangement) between the corresponding atoms.

In the top spectrum of Figure 8 ($\tau_m = 100$ ms), where the exchange is complete, we observe both types of cross-peaks. The two sets of off-diagonal peaks lying along lines parallel to the main diagonal belong to the first category and indicate that the process indeed involves overall molecular reorientation. More important are the hetero cross-peaks linking between the signals of the two nonequivalent C−H carbons. These signals

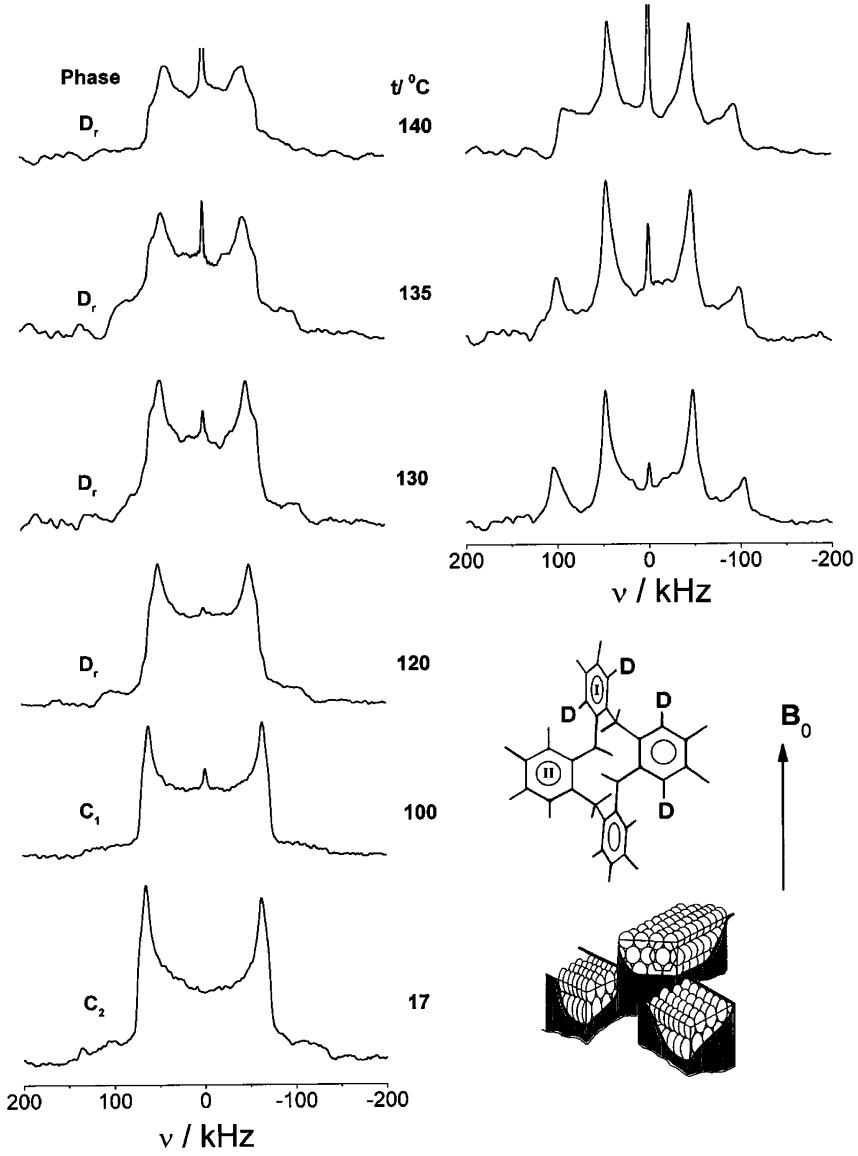

Figure 6. Deuterium NMR spectra of a TBC-9-d_8 sample (specifically deuterated at the aromatic carbons, 2) at the indicated temperatures and phases. The spectra were recorded by the quadrupole echo method with a 15 μs delay between the $\pi/2$ pulses. Recycle time, 0.3−3 s; number of scans, 6000−170 000. Left: Spectra obtained on heating a powder sample from the solid. Top right: Spectra of an aligned sample obtained by slow cooling from the melt. Bottom right: Schematic diagram of the planar distribution of domains obtained by aligning columnar phases in a magnetic field. The preferred orientation of a TBC-*n* molecule in an aligned column (C_2 ||B_0) is also displayed.

are shown on an expanded scale in the diagrams on the right-hand side of the figure. They confirm that the molecular reorientation indeed involve pseudorotation. No cross-peaks can be observed between the nonequivalent C−C and C−O carbons because they are not resolved in the mesophase spectra. Similarly, no resolved cross-peaks were observed for the α-methylene doublet in this experiment, but very clear cross-peaks were detected when the experiment was repeated at a higher magnetic field (201 MHz). The two bottom spectra in Figure 8 were recorded with mixing times of 10 ms and 1 ms. A clear decrease in the relative intensities of the cross-peaks with decreasing τ_m can be observed. From these spectra alone, it is difficult to derive accurate kinetic parameters for the pseudorotation/rotation process. They, however, provide an estimate of about 3−5 ms for its correlation time (at 124 °C), in agreement with the more detailed measurements discussed in the next section. This is also consistent with the claim made in connection with Figure 5 that at 116 °C there is negligible contribution (<25 Hz) to the line width from dynamic processes.

4.3. Analysis of the Dynamic MAS Spectra. To determine the kinetic parameters of the pseudorotation/rotation process, we attempt a quantitative analysis of the line shapes of the dynamic MAS spectra of Figure 7. The theory for simulating such line shapes was discussed in several earlier publications, and the method has been extensively used to study dynamic processes in solids and in liquid crystals, using particularly carbon-13 NMR.[3,26−28] We shall therefore not discuss the background theory of the method except to emphasize that its implementation requires detailed knowledge about the magnetic tensors of the exchanging/reorienting nuclei in the molecular frame. In the present case, these are the chemical shift tensors of the various aromatic carbons in the TBC-9 moiety. We assume that the average structure of the molecules (over the rapid librations) is that of a perfect sofa with C_{2h} symmetry. We also assume that the principal components of the chemical shift tensors of the aromatic carbons are as determined in the low temperature region of the mesophase (Table 1), but we slightly modify the isotropic chemical shifts of the C−C and

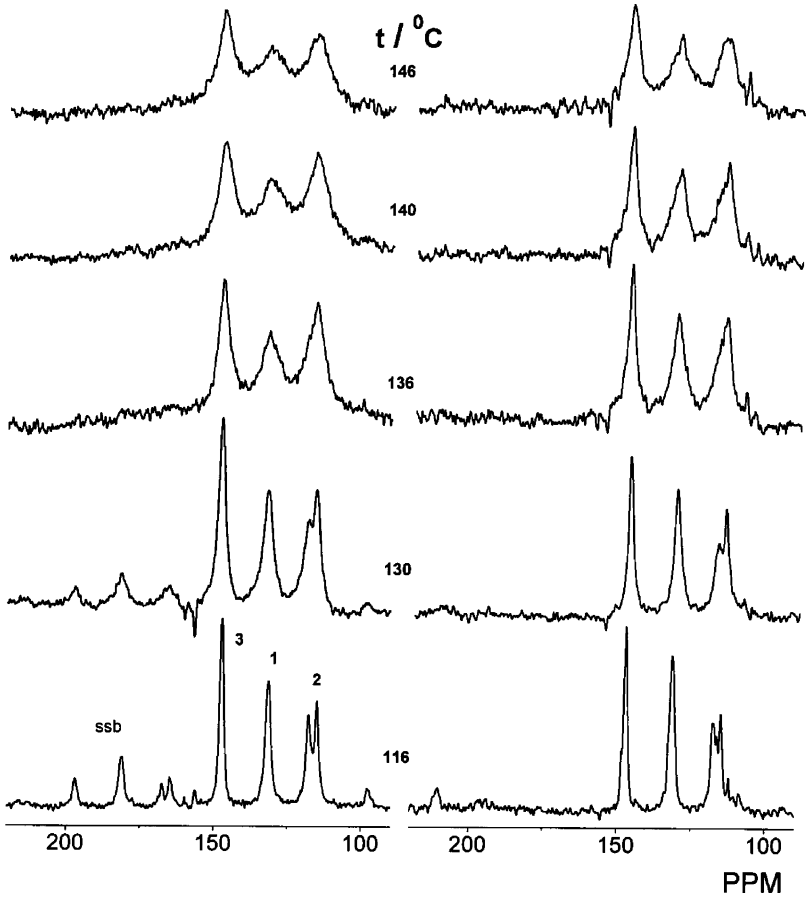

Figure 7. Carbon-13 MAS NMR spectra of TBC-9 as a function of the temperature recorded at 75.47 MHz with a spinning rates of 3.75 kHz (left) and 6.0 kHz (right). Only the aromatic region of the spectrum is shown. Recycle time: 5 s; number of scans, 500−10 000.

C−O carbons, so that the differences between the corresponding pairs is as determined in the low-temperature isotropic solution (1.0 and 0.5 ppm, respectively). For the calculations, the chemical shift tensors of the exchanging carbons need to be written in a common molecular frame (MF). We take this frame to be as shown in the left side of Figure 2b, with *z* normal to the flat part of the sofa, *y* parallel to the C_2 symmetry axis, and *x* perpendicular to both. We also assume that the two types of benzene rings (in the flat and perpendicular parts) are exactly normal to each other. To write the chemical shift tensors in this frame, δ^{MF}, the anisotropic chemical shifts of the PAS, δ^{PAS}, were transformed with an appropriate transformation matrix

$$\delta^{MF} = R(\alpha, \beta, \gamma)\delta^{PAS}R(\alpha, \beta, \gamma)^{-1}$$

where α, β, and γ are Euler angles. These are given for the various carbons in Table 2, where the label I refers to the benzene rings in the flat part of the sofa and II to the perpendicular rings.

Using these anisotropic chemical shift parameters and an exchange independent width of $1/\pi T_2 = 100$ Hz, we simulated the dynamic MAS NMR spectra for each of the three pairs of aromatic carbons over a wide range of rates, *k*, of the pseudorotation/rotation process. In these calculations, a total of 7−11 ssb were included, depending on the spinning rate. The final spectra were obtained as superposition over 538 different crystallite orientations in the rotor, chosen according to the method of Conroy.[29] The (full) line widths (at half-maximum height) of the center band signals of the simulated spectra (for three spinning frequencies), so obtained, are plotted in Figure 9 as a function of *k*.

The main features of such curves have been discussed earlier.[28] If the difference in δ_{iso} between the exchanging sites is small compared to $\Delta\delta$, the lines first broaden, pass through a maximum, and then narrow again. The maximum broadening is largest for the carbons with the largest $\Delta\delta$, and its magnitude decreases with increasing the spinning rate. The maximum occurs when $k \approx 2\pi\nu_R$, where ν_R is the spinning frequency. The initial broadening is larger for slower spinning, but the exchange narrowing is independent of ν_R. The curves for the C−H carbons start at $k = 2 \times 10^3$ s^{-1}, because at slower rates the spectrum is an unresolved doublet and there is no meaning to measuring the full line width. The slight initial decrease in the line width for the C−C carbons is due to the effect of the small (unresolved) chemical shift difference between the exchanging carbons.[28]

It is clear from the evolution of the spectra in Figure 7 that they correspond to the broadening regimes of the line width curves (Figure 9). Thus, by comparing the experimental line widths with the broadening branches of the calculated curves, the exchange rates can be determined. This we have done for the three aromatic carbons for the two spinning rates measured. The final analysis was, however, limited to the 6 kHz spectra because of their better quality. The results, averaged over the three carbons, are plotted in Figure 10.

The results lie on a smooth curve, lending support to the procedure used. On the other hand, the analysis suffers from the fact that it relies on just the fitting of the line width, rather than the full line shape. In the slow regime, we also tried to fit the shape of the C−H doublet. However, as may be seen in Figure 7, the broadening of the two components is quite different, most likely because their anisotropic tensors are not

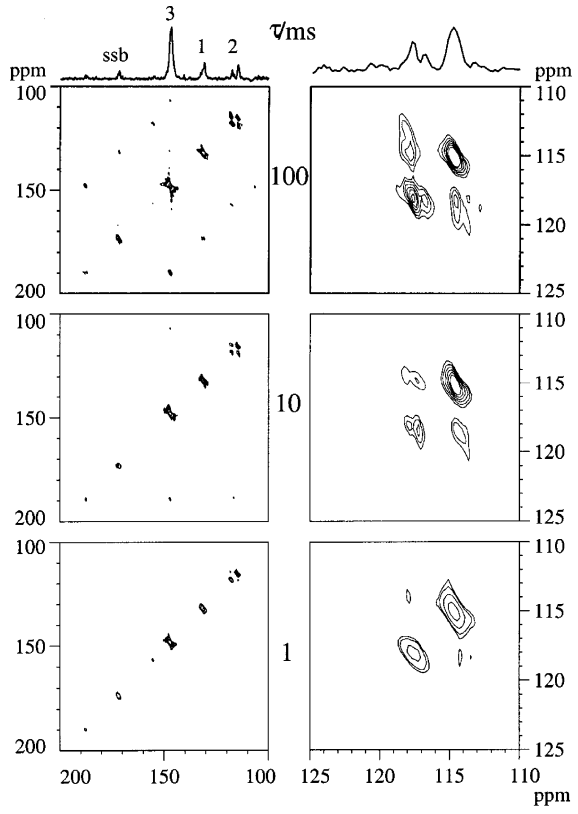

Figure 8. Carbon-13 rotor-synchronized 2D exchange (magnitude) spectra of TBC-9 for the indicated mixing times, τ. The spectra were recorded at 75.47 MHz. Those on the left show the full aromatic region. Expanded spectra of the C−H carbon are shown on the right. The 1D traces at the top are projections of the upper 2D spectra. Recycle time, 5 s; CP contact time, 2 ms; number of t_1 increments, 100−115, 65.4 μs apart; total number of scans, 100−300; dwell time in t_2, 32.7 μs; number of acquisition points, 1024.

TABLE 2: Euler Angles Relating the Principal Axis System (PAS) to the Molecular Frame (MF) for the Various Aromatic Carbons of TBC-9 (see Figure 2)

benzene ring	I			II		
Euler angle	α	β	γ	α	β	γ
C−C	−60	0	0	−30	−90	180
C−H	0	0	0	−90	−90	180
C−O	60	0	0	30	90	180

exactly the same, as assumed in the calculation. Also, from the packing heterogeneity discussed, in section 4.1, we could anticipate a distribution of correlation times for the pseudorotation/rotation process, which was not taken into account in the analysis.

Finally, it is clearly noticed that the plot in Figure 10 is not straight, as would be expected for an Arrhenius behavior. Rather, it appears to bend down at higher temperatures. We believe that this is an artifact resulting from our using fixed values for the components of the anisotropic chemical shift tensors. We have seen that within the mesophase region the asymmetry parameter of the deuterium quadrupole tensor (of the aromatic C−D deuteron) increases with increasing temperature, and we attributed the effect to increase in the librations amplitude. The same motion should also reduces the chemical shift anisotropy of the aromatic carbons. As discussed above, the exchange broadening increases with $\Delta\delta$, so that by using the low-temperature values we, in fact, undervalue k. Because of lack of knowledge about the temperature dependence of the carbon chemical shift tensors, we are unable to quantitatively correct for this effect. However, we can still reliably use the low-temperature data to estimate kinetic parameter for the process. Taking the initial slope of the curve in Figure 10, we obtain

$$\log(A/s^{-1}) = 28; \quad \Delta E = 250 \text{ kJ/mol}$$

We note that the activation energy is considerably higher than expected for a process that merely involves pseudorotation and rotation within a columnar liquid crystal. Also, the preexponential factor is orders of magnitude higher than expected from absolute rate theory. Such extreme values for the activation parameters are sometimes interpreted in terms of cooperative processes. In the present case, this would mean that a segment of the column, involving a number of molecules, reorients in concert. However, the presence of pseudorotation clearly indicates that the process involves single molecules because a cooperative reorientation does not require sofa-sofa interconversion. We therefore prefer to explain the high values of the Arrhenius parameters in terms of a temperature-dependent barrier to rotation within the columns.[30] If we assume that this barrier decreases with increasing temperature, it would effectively result in a steeper k vs $1/T$ curve than expected from the Arrhenius equation with constant ΔE. Similarly, large Arrhenius parameters have been observed in several other columnar mesophases.[3,31] This is perhaps not surprising because in such phases the thermal expansion of the columns may effectively reduce the packing potential which holds the molecules in place.

4.4. Alignment of the Mesophase in a Magnetic Field. Columnar discotic mesophases with flat aromatic cores usually align in a magnetic field with the columnar axes normal to the field direction.[32] This results in a planar distribution of domains whose directors are distributed in a plane perpendicular to the field direction (see diagram on the bottom right of Figure 6). This is a consequence of the anisotropic magnetic susceptibility of aromatic moieties, which prefers $\chi_{||}$ (normal to the aromatic plane) to align perpendicular to the field direction. Kuebler et al.[9] have shown that the same also applies to the flexible sofa conformation of the TBC-7 mesophase. In this case, however, the alignment is 2-fold; the columns align perpendicular to the magnetic field and within the columns the molecules are oriented such that their C_2 symmetry axes align parallel to the field direction as shown in the bottom right diagram of Figure 6. This alignment ensures that both types of benzene rings (I and II) of the sofa conformation are oriented with their normals perpendicular to the magnetic field. Indeed when a melt of TBC-9-d_8 is slowly cooled within the magnetic field into the mesophase and the deuterium spectrum recorded a line shape typical of an aligned sample is obtained (see upper right side of Figure 6). In particular, we note two doublets, an outer and an inner one, which we associate, respectively, with the C−D deuterons in rings II (C−D bonds parallel to B_0) and in rings I (perpendicular to B_0).

Similar alignment features are also observed in the carbon-13 spectra of static (nonspinning) samples. Examples of such spectra are shown in Figure 11.

The bottom trace in this figure is due to a solid powder. The relatively strong and narrow peak at high field (below 100 ppm) is due to the aliphatic α carbons, whereas the broad signal ranging from the aliphatic peak to 230 ppm is due to the aromatic carbons. Trace b corresponds to the same sample after heating to the mesophase (at 117 °C). The range of the chemical shift of the aromatic carbons is now reduced to 30−200 ppm, with a clear edge at the latter end. This is consistent with the reduced chemical shift anisotropy observed in the mesophase (see Table 1). Finally, trace c is due to an aligned mesophase

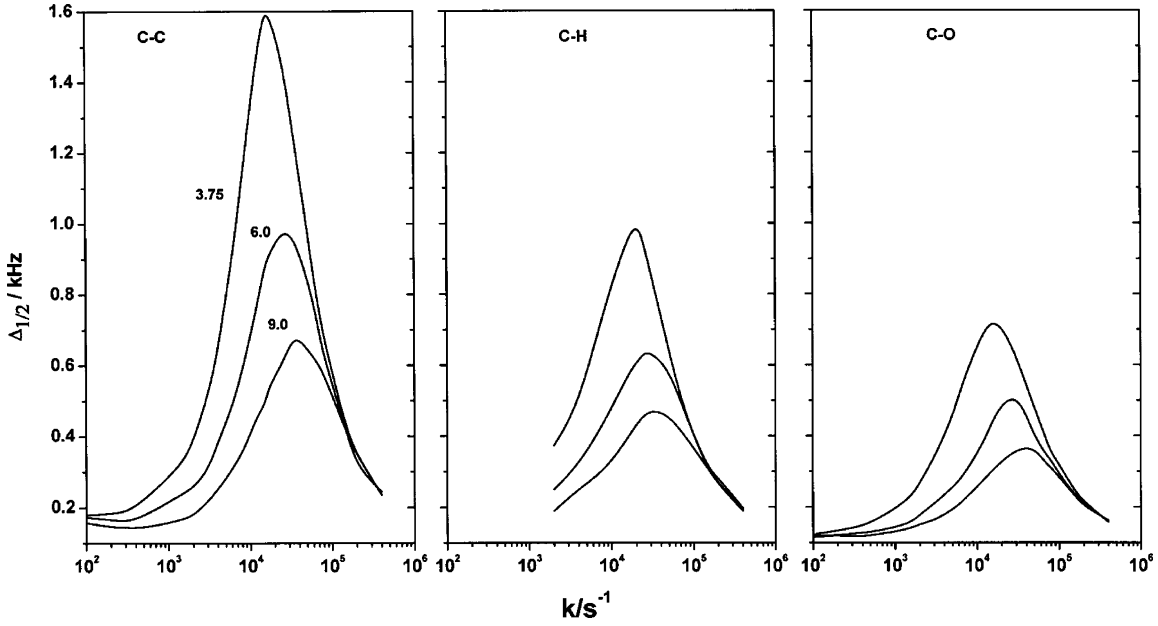

Figure 9. Plots of the calculated full width, $\Delta_{1/2}$, at half-maximum height (in kHz) of the dynamically broadened center signals of the aromatic carbons in the MAS spectra of TBC-9 as a function of the rate, *k*, of the pseudorotation/rotation process. Plots are given for the three rates of sample spinning (ν_R) as indicated in the left diagram. For the calculation, an exchange independent width of $1/\pi T_2 = 100$ Hz was assumed.

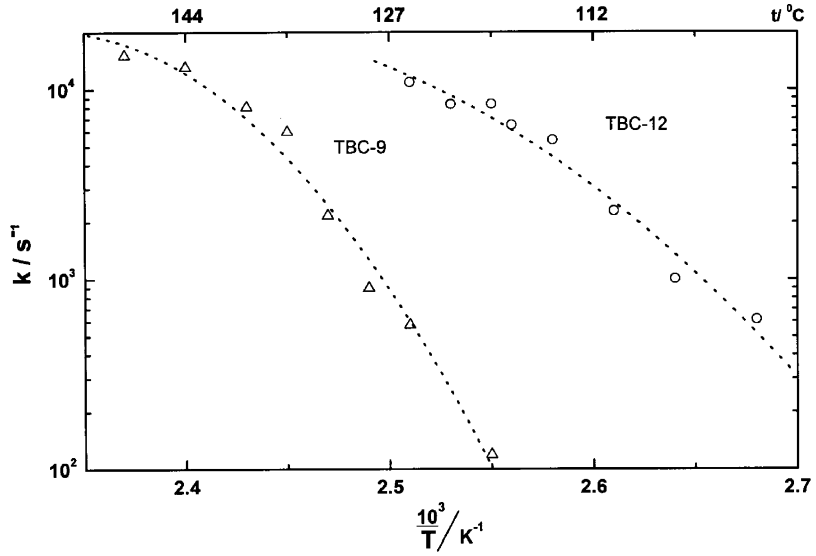

Figure 10. Plots of the pseudorotation/rotation rates as a function of the reciprocal absolute temperature in the mesophases of TBC-9 and TBC-12. The rates were derived from experimental CPMAS carbon-13 spectra recorded at 6 kHz and 9 kHz, respectively, using the theoretical curves shown in Figure 9.

(also at 117 °C) obtained by slow cooling from the melt in a magnetic field. There is essentially no intensity in the high-field region corresponding to benzene rings normal to the magnetic field ($\delta_{iso} + \delta_{33}$). Instead there is an intense signal in the range ($\delta_{iso} + \delta_{11}$) to ($\delta_{iso} + \delta_{22}$), corresponding to benzene rings parallel to B_0. The resolution of this spectrum is quite poor compared to that of the deuterons described above. This is due to the multitude of nonequivalent carbons contributing to the signal and the wide range of in-plane chemical shift anisotropy. However, the main features of alignment can still be recognized.

5. Results for TBC-12

5.1. Deuterium NMR Spectra. The TBC-12 homologue exhibits in addition to a Dr phase also a high-temperature hexagonal phase, Dh. The transition between the two phases is weakly first order, involving a small adjustment of the lattice parameter from that of center-rectangular (*C*2*mm*) to hexagonal (*p*6*mm*). When thin specimens are examined by optical microscopy, the Dr ↔ Dh transition is clearly observed; however, X-ray measurements (of more bulky samples) showed a wide range of coexistence of the two phases.[6] It is likely (but not confirmed) that this wide range also includes an intermediate oblique phase as was found for the TBC-13 homologue.[7] At any event, a similar wide biphasic range is also observed in the deuterium NMR of a TBC-12-d_8 sample (see Figure 12). The spectra of the solid phases and the Dr phase (at its low-temperatures range) are similar to the corresponding spectra in TBC-9-d_8 (see Figure 6).

As the transition to the Dh mesophase is approached, a wide range of biphasic regions is obtained (see traces corresponding to 115 and 120 °C), exhibiting signals from both the Dr and Dh phase. Spectra of neat Dh can only be observed over a narrow temperature range (see spectrum at 125 °C), because of

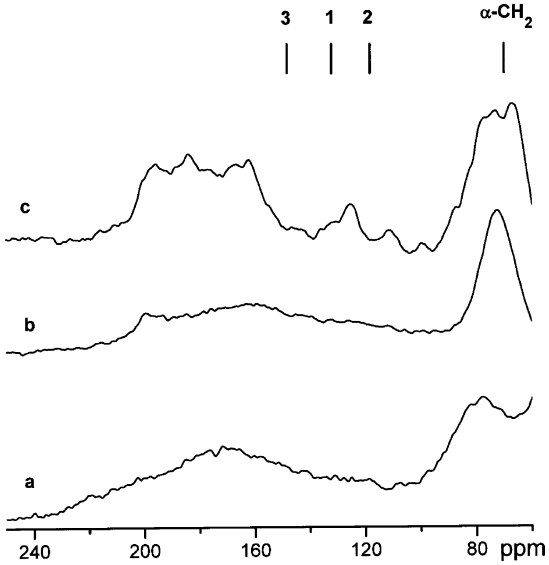

Figure 11. Carbon-13 spectra (recorded at 75.47 MHz) of a static (nonspinning) sample of TBC-9. (a) Solid powder (C_1) at 20 °C. (b) Nonaligned mesophase at 117 °C. (c) Aligned mesophase at 117 °C. The bars at the top indicate the positions of the aromatic and α-methylene peaks in the melt.

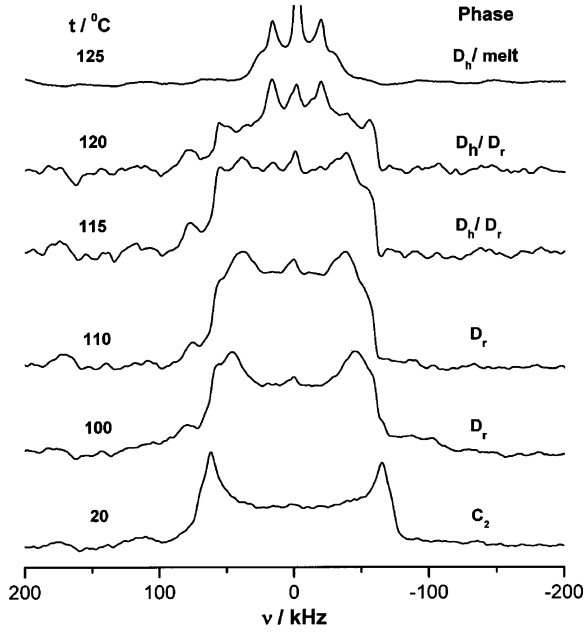

Figure 12. Deuterium NMR spectra of TBC-12-d_8, obtained by heating from the solid. Note the wide biphasic (Dr/Dh and Dh/melt) ranges.

the appearance of the center peak due to (a small amount of) the isotropic melt, as the clearing temperature is approached. The signal of the Dh phase is much narrower than that of Dr and highly biaxial ($\nu_Q = 46$ kHz, $\eta = 0.22$). The carbon-13 MAS spectra to be discussed shortly do not indicate any dynamic discontinuity at the Dr ↔ Dh transition. We therefore believe that these changes in the deuterium quadrupole parameters reflect an increase in the libration amplitude of the sofa conformer on passing into the Dh mesophase. Apparently, the higher local symmetry around the columns in the latter phase allows for higher distortions of the sofa structure.

In this connection, it is interesting to note that on slow cooling the melt of TBC-12 into the hexagonal phase no alignment of the mesophase is observed. This is not surprising in view of the fact that in the Dh phase the transverse orientations (the directions of the C_2 axes) of the columns are not correlated, as they apparently are in Dr. Consequently, the anisotropic magnetic susceptibility of the phase is fairly small, and only very little alignment torques are felt by the domains in the magnetic field. On further cooling through the Dh → Dr transition, the sample does align, yielding spectra similar to those of TBC-9-d_8, when cooled from the melt (Figure 6).

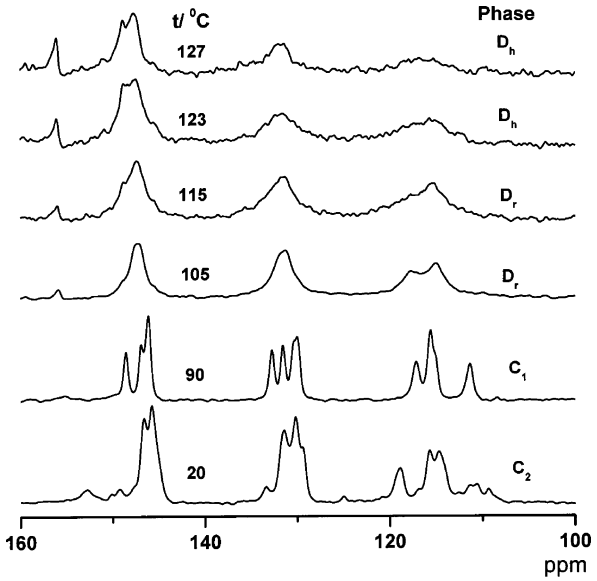

Figure 13. Dynamic carbon-13 MAS NMR spectra (aromatic carbons only) of TBC-12 as a function of the temperature in the Dr and Dh mesophases. $\nu_R = 9.0$ kHz; $\nu_L = 75.47$ MHz.

5.2. Carbon-13 MAS Spectra. Carbon-13 MAS NMR spectra of a TBC-12 sample in the solid and columnar phases are shown in Figure 13. The spectra in the solid phases are similar to those observed in TBC-9, but less resolved. Likewise, the melting of the solid leads to a single-species spectrum similar to that observed for the Dr mesophase in TBC-9.

There are three aromatic bands due to the three types of aromatic carbons. The lines are broadened due to chemical shift heterogeneity, so that only the larger splitting due to the C−H carbons is resolved. On further heating, the lines gradually broaden until the clearing point of the Dh phase. The spectra shown in Figure 13 were recorded by CP-MAS. When recorded by single pulses, sharp peaks due to the isotropic melt are observed well below the reported clearing transition. These isotropic signals are not observed when recorded by the CP-MAS method. No discontinuity in the line width is observed at the Dr to Dh transition, but we should recall that the transition involves a wide biphasic region. There are two vexing peaks at the low-field end of the spectrum. We finally discovered that the one at 147 ppm forming the shoulder on the C−O peak is a ssb of the major peak due to the aliphatic carbons, whereas the one at 155 ppm could not yet be assigned.

We have interpreted the dynamic MAS spectra of TBC-12 in much the same way as for TBC-9. The results are plotted in Figure 10. We observe again a leveling off of the curve with increasing temperature, which we ascribe to us disregarding the reduction in the carbon-13 chemical shift anisotropy. If the initial slope is considered, the following kinetic parameters are derived:

$$\log(A/s^{-1}) = 18; \quad \Delta E = 165 \text{ kJ/mol}$$

6. Summary and Conclusions

Earlier studies have shown that deuterium NMR is a most powerful tool for the study of discotic columnar mesophases.

In the present work, we have explored the suitability of carbon-13 MAS NMR to study these systems. The method has the advantage that it does not require isotopic labeling, is site selective, and can therefore report on both overall molecular motions as well as conformational rearrangement. The method is sensitive to a dynamic window that is often not accessible by other methods. The quantitative analysis of the data is, however, complicated by the fact that the chemical shift tensors, required for the quantitative analysis, are not always accurately known. Nevertheless, we were able to provide new information on the columnar phases of the TBC-*n* series, whose homologues consist of a nonplanar, flexible core. Thus, by using 2D exchange, it was possible to confirm that the molecular reorientation within the column indeed involves sofa-sofa rearrangement as suggested by Kuebler et al.[9] By analyzing the dynamic line broadening, rate constants could be determined over wide dynamic ranges. Comparing the data of three homologues of the TBC-*n* series shows that the rate of the reorientation increases with the length of the side chains, demonstrating their role in providing "lubrication" for the process. Thus, for the three homologues with $n = 7$,[9] 9, and 12, the temperature at which the reorientation rate is 10^3 s^{-1} corresponds to 160, 130, and 100 °C, respectively. The temperature at which pseudorotation in solution has this rate is less than 40 °C, demonstrating the hindering effect of the molecular stacking on the rearrangement process.

The high resolution of the carbon-13 MAS spectra also made it possible to detect the presence of a chemical shift distribution that probably reflects stacking dispersion within the columns. In principle, this dispersion could be estimated by using a suitable theory that takes into account the effect of neighboring molecules on the carbon chemical shift.

References and Notes

(1) Cammidge, A. N.; Bushby, R. J. Synthesis and structural features. In *Handbook of Liquid Crystals*; Demus, D., Goodby, J., Gray, G. W., Spiess, H. W., Vill, V., Eds.; Wiley-VCH: New York, 1998; Vol. 2B, Chapter VII, pp 693−748.

(2) Poupko, R.; Luz, Z.; Spielberg, N.; Zimmermann, H. *J. Am. Chem. Soc*. **1989**, *111*, 6094−6105.

(3) Zimmermann, H.; Bader, V.; Poupko, R.; Wachtel, E. J.; Luz, Z. *J. Am. Chem. Soc*. **2002**, *124*, 15286−15301.

(4) Zimmermann, H.; Poupko, R.; Luz, Z.; Billard, J. *Liq. Cryst*. **1988**, *3*, 759−770.

(5) Zimmermann, H.; Poupko, R.; Luz, Z.; Billard, J. *Liq. Cryst*. **1989**, *6*, 151−166.

(6) Spielberg, N.; Sarkar, M.; Luz, Z.; Poupko, R.; Billards, J.; Zimmermann, H. *Liq. Cryst.* **1993**, *15*, 311−330.

(7) Dai, S.; Spielberg, N.; Zimmermann, H. *Mol. Crys. Liq. Crys*. **1997**, *303*, 97−101.

(8) Kranig, W.; Spiess, H. W.; Zimmermann, H. *Liq. Cryst.* **1990**, *7*, 123−129.

(9) Kuebler, S. C.; Boeffel, C.; Spiess, H. W. *Liq. Cryst.* **1995**, *18*, 309−318.

(10) Maliniak, A.; Luz, Z.; Poupko, R.; Krieger, C.; Zimmermann, H. *J. Am. Chem. Soc*. **1990**, *112*, 4277−4283.

(11) Kuebler, S. C. Ph.D. Dissertation, Gutenberg University: Mainz, 1996.

(12) Khetrapal, C. L.; Raghothama, S.; Suryaprakash, N.; Kunwar, A. C. *Liq. Cryst.* **1988**, *3*, 413−415.

(13) Akai, T.; Shimizu, Y. *Liq. Cryst.* **2000**, *27*, 437−441.

(14) Fischbach, I.; Pakula, T.; Minkin, P.; Fectenkötter, A.; Müllen, K.; Spiess, H. W. *J. Phys. Chem. B* **2002**, *106*, 6408−6418.

(15) Dvinskikh, S. V.; Luz, Z.; Zimmermann, H.; Maliniak, A.; Sandström, D. *J. Phys. Chem. B* **2003**, *107*, 1969−1976.

(16) Werth, M.; Leisen, J.; Boeffel, C.; Dong, R. Y.; Spiess, H. W. *J. Phys. II France* **1993**, *3*, 53−67.

(17) White, J. D.; Gesner, B. D. *Tetrahedron* **1974**, *30*, 2273−2277.

(18) Kalinowski, H. A.; Berger, S.; Braun. S. *Carbon-13 NMR Spectroscopy*; Wiley: New York, 1988; Chapter 3.

(19) Burlinson, N. E.; Ripmeester, J. A. *J. Incl. Phenom.* **1985**, *3*, 95−98.

(20) de Gennes, P.-G. *J. Physique—Lett.* **1983**, *44*, 657−664.

(21) Herzfeld, J.; Berger, A. F. *J. Chem. Phys*. **1980**, *73*, 6021−6030.

(22) Duncan, T. M. *Principal Components of Chemical Shift Tensors: A Compilation*, 2nd ed.; The Farragut Press: Madison, WI, 1997.

(23) de Jong, A. F.; Kentgens, A. P.; Veeman, W. S. *Chem. Phys. Lett.* **1984**, *109*, 337−342.

(24) Titman, J. J.; Luz, Z.; Spiess, H. W. *J. Am. Chem. Soc*. **1992**, *114*, 3756−3765.

(25) Luz, Z.; Spiess, H. W.; Titman, J. J. *Isr. J. Chem*. **1992**, *32*, 145−160.

(26) Schmidt, A.; Vega, S. *J. Chem. Phys*. **1987**, *87*, 6895−6907.

(27) Luz, Z.; Poupko, R.; Alexander, S. *J. Chem. Phys.* **1993**, *99*, 7544−7553.

(28) Reichert, D.; Hempel, G.; Zimmermann, H.; Schneider, H.; Luz, Z. *Solid State NMR* **2000**, *18*, 17−36.

(29) Conroy, H. *J. Chem. Phys*. **1967**, *47*, 5307−5318.

(30) Müller, A.; Haeberlen, U.; Zimmermann, H.; Poupko, R.; Luz, Z. *Mol. Phys.* **1994**, *81*, 1239−1258.

(31) Zamir, S.; Luz, Z.; Poupko, R.; Alexander, S.; Zimmermann, H. *J. Chem. Phys.* **1991**, *94*, 5927−5938.

(32) Goldfarb, D.; Luz, Z.; Zimmermann, H. *J. Phys.* **1981**, *42*, 1303−1311.